

Chapter 7

VACUUM SYSTEM

7.1 Introduction

Beam stability and beam lifetime are the major requirements for good operation of the synchrotron light sources. Pressures in the range of low 10^{-9} mbar are typical values to be achieved in order to have a good beam lifetime, the pressure inside the vacuum chamber is produced by the thermal desorption and the photon stimulated desorption processes, the interaction between the electron beam with the residual gases leads to an elastic and inelastic scattering causing electron loses and reducing the lifetime of the beam.

To achieve the required values of the pressure, a good vacuum system need to be designed; good and efficient pumping system, good monitoring, good choice of vacuum chamber design and materials and an efficient cleaning and conditioning all will lead to low outgassing and low pressure.

7.2 SESAME Parameters

General characteristics of the machine, which are the most important from vacuum point of view, are tabulated in Table (7.1):

Table 7.1: SESAME main parameters.

Beam energy (GeV)	2.5
Maximum beam current (mA)	400
Horizontal emittance (nmrad)	24.3
Number of dipoles	16
Circumference (m)	124.8
Bending radius (m)	5.95643
Dipole magnetic length (m)	2.339
Dipole magnetic field (T)	1.4
Electron beam vacuum chamber vertical / horizontal aperture (mm)	30 / 70
Distance between two dipoles LSS / SSS (m)	5.552 / 5.370

Others like photon flux, average pressure...etc will be calculated later on.

7.3 Requirements

The vacuum system must be designed in a way, which will guarantee that the following requirements must be taken into consideration:

- An average dynamic pressure of $1 \cdot 10^{-9}$ mbar must be achieved by the end of the conditioning stage, such a value for the pressure will allow a good beam lifetime of not less than 14 hours to be obtained. Good optimisation of the locations and the sizes of the pumps will assure that such values of pressure to be achieved.
- The electron beam must see a smooth surface to avoid the interaction of the electromagnetic field of the electron beam with the vacuum chamber walls, as this will produce wake fields which are sources of energy spread and sometimes killing the beam, Hence the electrical impedance of the vacuum chamber must kept minimal and constant around the ring.
- Sufficient cooling, to dissipate the heat load associated with the synchrotron radiation as high power in the vacuum chamber walls will enhance thermal desorption and will

increase photon induced desorption, also the high power will cause thermal expansion of the vacuum chamber. Sufficient cooling will be by the good design of the crotch absorbers as well of the distributed absorbers.

- The physicists' requirements must be considered, like small vertical dimension of the vacuum chamber to get a small distance between the magnet poles, another requirement is (and as mentioned before) an electrical continuity to avoid RF resonance.
- Good and sufficient monitoring is required as achieving the required pressure is as much important as measuring that pressure precisely.
- The vacuum system must be flexible for upgrading and other future changes, also it needs to be designed with reasonable cost for example by providing the machine with equipments which are available in the market not specially manufactured for SESAME.

7.4 General Layout

SESAME storage ring has 8 identical cells, see figure (7.1), each cell is divided into two sections: the straight section which is dedicated for the insertion devices, RF cavities and injection septum magnet, see figure (7.2). The second part is the arc, which contains the achromat section (the magnets region), this section contains the vacuum chamber through the dipoles, quadrupoles and sextupoles, see figure (7.3). The two parts are connected to each other by flanges, besides, bellows with RF fingers are placed by the ends of each straight to absorb the thermal expansion and compression in the storage ring and to allow easy installation during assembly.

From vacuum point of view, SESAME storage ring will be divided into 4 sections, separated from each other by RF shielded gate valves, so each part will include two cells, i.e. four dipoles and three straights. The valves are situated in the short straight sections: two gate valves by the end of each RF straight, another gate valve located by the end of the injection straight, and one at SSS IV-2 straight, see figure (7.4).

Lumped absorbers provided with vacuum pumps located close to them, will absorb the unwanted synchrotron radiation. The layout of the storage ring is described in more details in chapter 5.

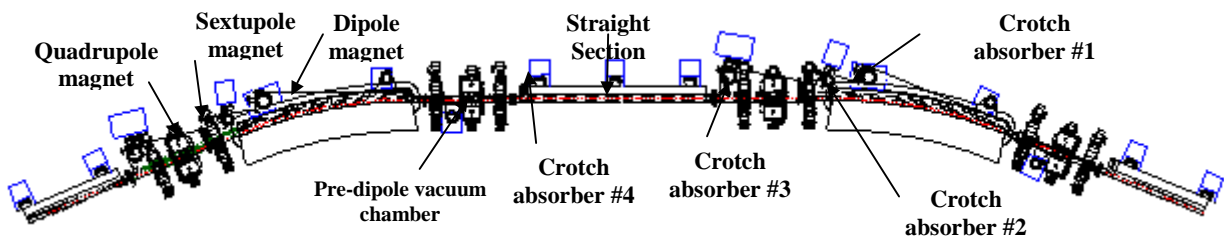


Figure 7.1 The unit cell of the storage ring.

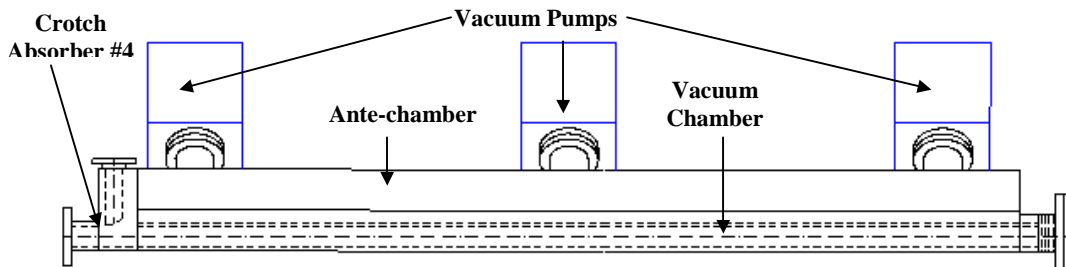


Figure 7.2: The straight section vacuum chamber.

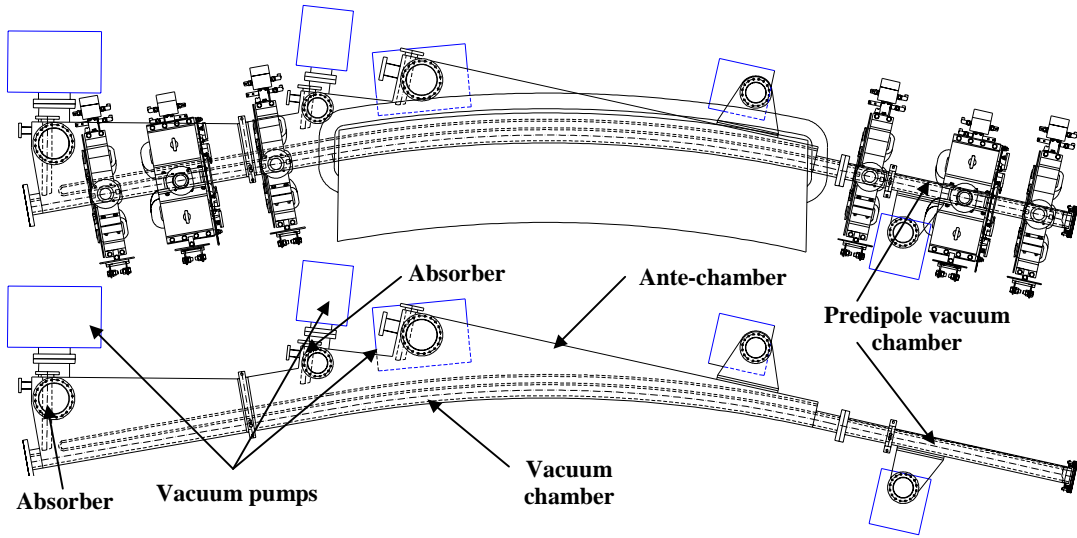


Figure 7.3: The achromat vacuum chamber.

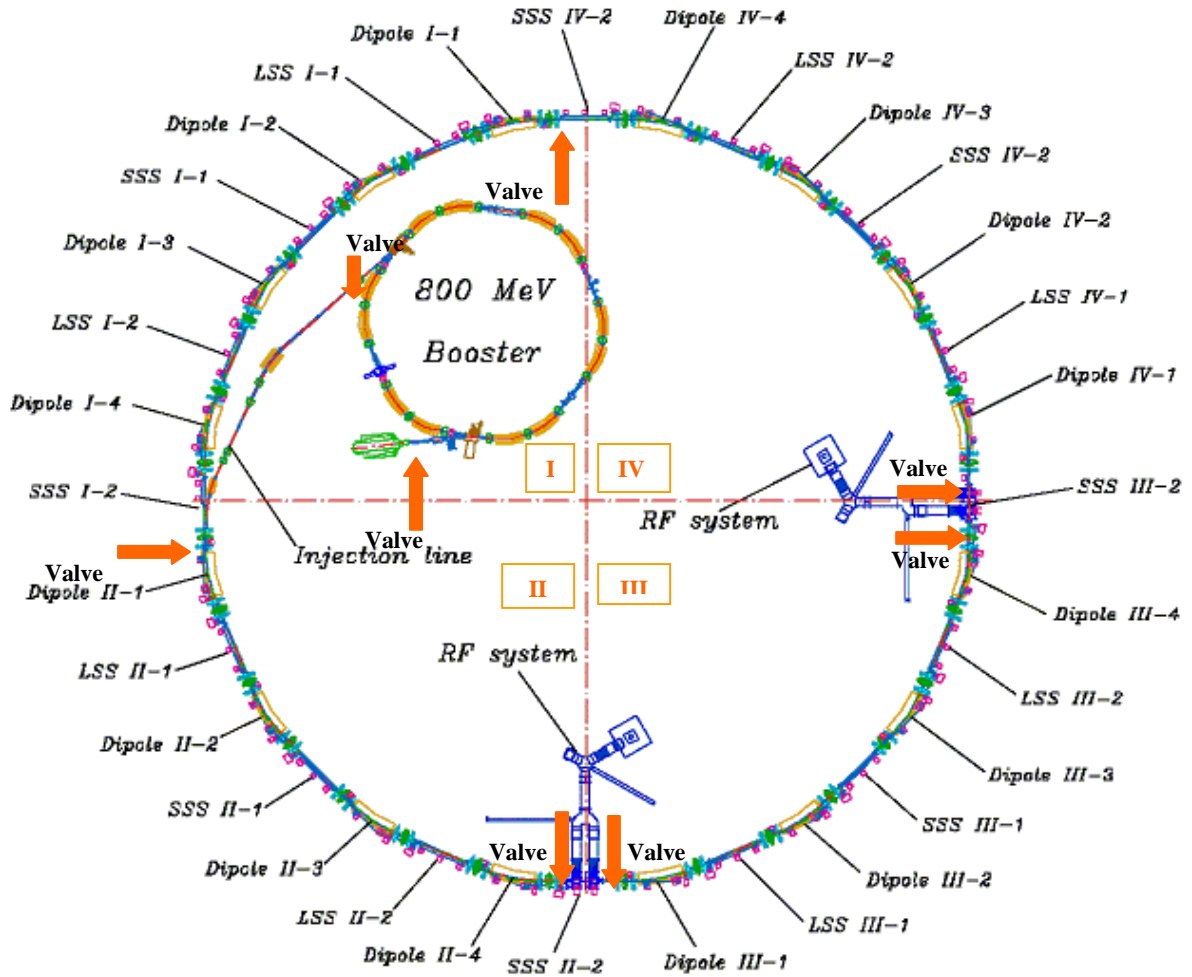


Figure 7.4: The locations of the valves distributed around the machine.

7.5 Materials for the Vacuum Chamber

In general, synchrotron light sources vacuum chambers are fabricated from the alloys of stainless steel, aluminium or copper. However copper is used inside the vessel as photon stopper or radiation absorbers, where high heat loads have to be dissipated.

The materials will be used for SESAME vacuum chamber must obey the vacuum and mechanical requirements, like the mechanical strength (stability and hardness), thermal conductivity, magnetic permeability, fabrication and joining...etc. [1], [2]

7.5.1 Proprieties

Unfortunately, there isn't one material that has all the required properties for synchrotron radiation sources' vacuum systems. So SESAME vacuum chamber will be fabricated from stainless steel (316LN) and OFHC copper will be used internally as synchrotron radiation absorber. The reasons for this choice are described here.

7.5.1.1 Vacuum Performance

The vacuum performance of the material can be expressed by the photon desorption yield and its variation with the beam dose, and also with the "memory effect" of the material.

Figure (7.5) shows the measured values of photon desorption yield and its variation with the beam dose for stainless steel, aluminium and copper, respectively, for different gases.

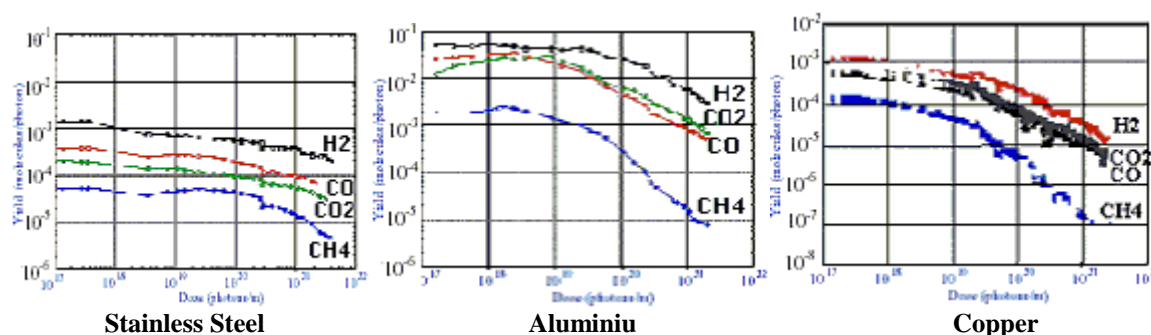


Figure 7.5: Photon stimulated desorption yield variation with accumulated beam dose for stainless steel, aluminium and copper, respectively. [1]

It is clear from the curves that the main difference between the three is that aluminium has higher values of photon desorption yield than stainless steel and copper, but this is only true in the early stages of conditioning, and after that all have almost similar values for the desorption yield for the different gases.

Another important property required for the material to be used in the vacuum systems of the synchrotron sources is to have a good "memory effect", i.e. the desorption yield for scrubbed vacuum chamber need to have lower value than that for unscrubbed chamber after being vented, stainless steel and copper have a better memory effect than that of aluminium. [2].

7.5.1.2 Mechanical Properties

Aluminium has good properties such as: it is easy for manufacturing by extrusion especially for long beam tubes and complex chambers, also it is completely non magnetic. However aluminium has several disadvantages such as it has weak mechanical properties and it is difficult for joining.

In the other hand, copper (OFHC copper) has good thermal conductivity but its production process is more complicated and expensive in comparison to aluminium and stainless steel (if copper is used for vacuum vessels with an antechamber, the chambers need to be extruded separately from the antechamber and welded together afterwards). [3]

Stainless steel (316LN alloy is usually used for UHV applications for synchrotron light sources) has good mechanical strength; it is easy to weld and has high hardness also 316LN stainless steel is corrosion resistance alloy. Besides stainless steel has a low magnetic permeability, so it can be used within magnets. The thermal conductivity of stainless steel is very poor in comparison to copper, therefore to transport high heat loads (e.g. in absorbers) copper plates need to be used. Also stainless steel can be baked out up to (350°C) to remove water and fired (up to 900°C) to reduce H₂, such temperature must not be reached during bake out for aluminium. [3], [4]

There are another two arguments for choosing the material for the accelerator's vacuum chamber:

- One should use a material, which can be handled by the accelerator laboratory and there exist expertise to deal with them.
- The vacuum system should be build by the industry, so manufacturers should have good experience with the material to be used.

For all of these reasons, stainless steel was the best choice for SESAME vacuum chambers because of its suitable properties and OFHC copper should be used for the absorbers because of its good thermal conductivity.

7.5.2 Flanges and Gaskets

Knife-edge flanges (CF-Conflat[®] Flanges) are used in many synchrotron light facilities, as they are available commercially in many different standard diameters. However, the standard CF flange has a small cavity, which increase the total impedance and local heating. This is can be solved by using a metal seal which will close the gap, another way is by changing the design to have a smaller gap, this problem can also be solved by using flat seal flanges which have no gap between it and the gasket, this type of flanges has another advantage, these flanges have smaller size than CF flanges, as a result less material being used for their production and then have a lower cost [3].

For the small circular vacuum pipes, ordinary CF will be used, and for the elliptical vacuum chambers in SESAME, VAT[®] seals (which have flat sealing surfaces) can be requested, experiments in some laboratories show their good performance. [5]

Silver coated copper gaskets will be used as they withstand the prebaking procedure before the final installation to the machine.

More detailed specifications for the flanges and the gaskets to be used for SESAME will be issued in the future.

7.6 Vacuum Chamber Design

The vacuum chamber can be divided into two sections; the achromat section which consists of the dipole vacuum chamber and sextupole and quadrupole magnets vacuum chamber, the second part is the straight section which is for the insertion devices, RF cavities and the injection septum. See figure (7.2) and (7.3).

The SLS approach have been adopted for SESAME vacuum chamber design, SESAME will be a full antechamber machine where synchrotron radiation will pass from the electron beam chamber through a slot to the antechamber towards the lumped absorbers located by the end of each antechamber section where large lumped pump is situated. [4], [6]

Concerning the introduction of the electrode of the BPM into the vacuum system, there are two methods have been adopted by the designers of the synchrotron light sources:

- Welding it directly to the BPM block.
- Using a separate flange to hold the electrodes, which are connected to the BPM block.

The BPM must be bolted rigidly to the magnet girders. To get rid of misreading of the BPM two options are available:

- The BPM electrode can be connected to the bellows to allow movement of the vacuum chambers.
- The movements of the vacuum chamber are detected by optical sensors and can be compensated for when reading the BPM. [4]

In order to avoid the extra cost of having a separate flange for the BPM the approach which will be adopted is to weld the BPM electrode directly to the BPM blocks and bolt it to the girders. The location of these BPM is shown in figure (7.6), one BPM will be located just before the dipole and one after the dipole magnet.

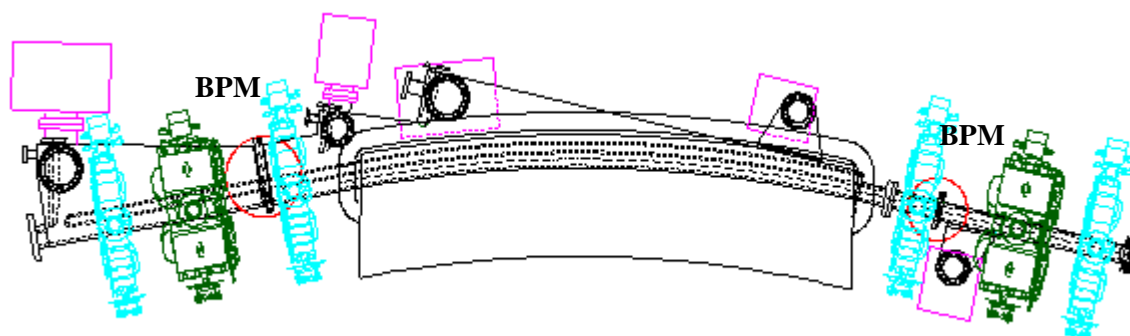


Figure 7.6: The locations of the beam position monitors.

Manufacturing should be done in such a way to eliminate trapped volumes (e.g. due to poor welding) to get better vacuum performance, since these volumes will increase the pump down time due to virtual leaks appearing. [7]

The detailed design of the vacuum chamber is represented in chapter 5.

7.7 Pumps Selection

7.7.1 Rough Pumping

The rough pumps are required to pump down the system from atmospheric pressure to below 10^{-6} mbar so that the UHV pumps can be started. The design should guarantee an efficient pumping and clean operation with the shortest possible time to reach the target pressure.

Mobile roughing stations are foreseen for SESAME, the main reason for this decision is to cut the cost of the roughing stations, as the number of the pumps required will be less in comparison to fixed stations, moreover, the use of mobile stations will save space in the storage ring, however, the use of mobile stations increases the cautions which need to be taken into consideration, especially the possibilities of contamination which are higher than if fixed stations being used, so control to the access of these pumps must be done to reduce these chances.

The roughing station consists of fore-vacuum pump and a turbomolecular pump.

The fore-vacuum pump will pump down from atmospheric pressure to 10^{-2} mbar so the turbomolecular pump can be switched on, if drag turbomolecular pump being used then its operation can be started at higher pressure (1mbar), this will reduce the time required for pumping down.

Diaphragm, piston or scroll pumps are possible types as baking pump for SESAME, but some characteristics will make one better than the others: time required to reach the target pressure, cost, the dimensions and the weight of the pump, noise level and if the pump has a

built in isolating valve to prevent the backstreaming to the system in case of a power failure, and above all the cleanliness of the pump, which must be in the acceptable levels for the vacuum system specifications.

Magnetic bearing turbomolecular pump (maglev turbo) is the best choice in term of cleanliness for our application for pumping down at high vacuum pressure, however, the cost of such pumps is about twice that for ceramic bearings turbomolecular pumps (also ceramic bearing turbomolecular pumps are mounted in a restricted orientation).

In case the manufacturer guaranteed that the percentage of the hydrocarbons in the system is in the acceptable limit (typically $< 1\%$ of the total pressure) then it is suitable to use these pumps, especially that new synchrotron light sources (e.g. SLS) are using such pumps without any noticeable problem.

Taking into consideration the conductance of the machine and as the conductance will limit the effective pumping speed of the pumps, it would be more sensible to use many pumps (and spread them around the cell) with a reasonable pumping speed rather than big pumps as this will reduce the pumping down time.

A pumping spout will be reserved near the first crotch absorber in the dipole to install the roughing station, it will be fitted with a 40mm aperture all metal valve. The station will also include a Pirani gauge, an inverted magnetron gauge and a let up valve.

The operation of the roughing stations will be manually. [8]

7.7.2 UHV Pumps

Capture pumps are the workhorse pumps required to achieve UHV in the vacuum systems for accelerators.

Ion pumps and titanium sublimation pumps are going to be used for SESAME; the reasons for this choice are described in this section.

The two types are clean pumps without any vibration (as they don't have any moving parts) also they do not need a valve to isolate them from the vacuum system. [9]

The ion pumps can be classified into three categories: the diode ion pump, the noble diode ion pump and the triode pump.

The diode ion pump is the standard sputter ion pump, which has a high pumping speed for all getter gases (and twice that of the triode ion pumps at 10^{-9} mbar) but this type of ion pumps has a very low pumping speed for noble gases (e.g. 2-5% of the pump pumping speed for Ar). Farther pumping, releases the previously buried noble gas molecules and as a result unstable pumping behaviour will be notice, this phenomena called (the instability of the noble gases).

The solution for this is either by using triode pumps or noble diode pumps; triode pumps will reduce the instability of the noble gases, the reason for this is the use of a negative voltage titanium grid instead of the ordinary cathodes, this approach will prevent the sputtering of the body or the anode as the energetic ions will not bombard the anode or the body of the pump, so the absorbed gases will stay bound on these surfaces.

Using noble diode pumps where the titanium cathode is replaced with tantalum cathode, will reduce the noble gases instability; the reason for this is that the instability depends on the reflection probability which is a function of the mass ratio of the ions species and the cathode material, so the instability will decrease as the atomic weight of Tantalum (181 AMU) is much higher than that of Ti (48 AMU). [10]

The replacement will not only reduce the instability but also will increase the pumping speed of the noble gases (about 20% of the pumping speed of air) but this will reduce the pumping speed of the active gases by 15% in comparison to the standard diode.

The titanium sublimation pump (TSP) is a very good solution for the need of high pumping speed at places of high outgassing rates. The pumping speed depends on the area being

coated with titanium, so special care need to be taken when designing the TSP envelope in order to guarantee the highest possible surface area to be covered by the filament material.

For pumping down SESAME, diode ion pumps will be used and few noble diode ion pumps will be distributed around the ring to reduce the noble gases (at least one for each cell), also titanium sublimation pumps will be used either as a separate pump or combined with the ion pumps and are going to be used in places with high outgassing, like near the crotch absorbers.

Concerning the operation range of the ion pumps, all the pumps must be able to operate at pressures from $5 \cdot 10^{-3}$ mbar down to $1 \cdot 10^{-10}$ mbar, but operation at pressures over 10^{-5} mbar need to be prevented, as this will decrease the life time of the pump. The titanium sublimation pumps must be conditioned and fired carefully taking into consideration that the pressure should not increase over $1 \cdot 10^{-7}$ mbar during the firing process, also ramping the power need to be in steps, so manual conditioning for the TSP is required. At 10^{-9} mbar pressure range, the TSP can be fired once every few days only.

The pumping ports of the pumps are of circular shape directly connected to the antechamber; as a result, there isn't any need for the use of RF screen to separate the pump from the system.

A recent approach in many synchrotron light sources is to bake out the ion pumps (also the TSP), so heaters need to be installed inside the body of the pump, this approach will not only decrease the conditioning time of the machine, but also it will be an advantage in case NEG ribbons being fitted to the pump (to increase the pumping speed) as this will activate the NEG. [11].

The power supplies for the ion pumps must be able to display the current, the voltage and the pressure as such information are very useful to estimate the pressure profile along the achromat.

The control units of the pumps must provide at least one relay set point for each HV channel, more detailed specifications for the ion pumps and the TSP control units and power supply units will be issued in the future. [12]

Newly designed machines adopted the NEG coating techniques in the design of the vacuum system like in Soliel and Diamond (also existing machines are replacing their old vacuum chambers with new coated like ESRF). NEG coating is a very good solution for systems having conductance limitations, but NEG coating required activation by heating, for non in-situ baked systems the activation of the NEG will be a problem, not only the activation of the NEG is the problem with this technique but also the high cost of the sputtering of the NEG material into the vacuum chamber. As for SESAME, this technology could be adopted for the small gap insertion devices as this will solve the limitation of the conductance, or installing NEG strips in the antechamber (with electrical feed through for activation) will provide a very good vacuum at these places.

7.8 Vacuum Instrumentation

The measurement of vacuum is as much important as providing the required vacuum, the total and partial pressure must be measured correctly. General specifications for both the total pressure gauges and the partial pressure gauges with the locations of the gauge heads throughout the facility are described here.

7.8.1 Total Pressure Gauges

As the total average dynamic pressure needs to be around $1 \cdot 10^{-9}$ mbar, then the gauges required for SESAME should be able to read a pressure of $1 \cdot 10^{-10}$ mbar which is the pressure

required before the beam being injected. The injector pressure measurement system requires a reliable reading down to $1 \cdot 10^{-9}$ mbar.

Unfortunately, it is not possible to cover the whole pressure range with a single gauge; a gauge is required to cover the low vacuum range (from atm. pressure to 10^{-3} mbar) such a gauge will be useful to provide reading during pumping down the system and during vacuum failure. A second gauge is required for UHV readings (for ranges of 10^{-3} - 10^{-10} mbar).

For low vacuum range, since the reading is just required to give an indication of the general situation of the vacuum system, so a gauge such as Pirani gauge is a good choice, as it covers the range from atm. to 10^{-3} mbar. The gauge should be bakeable up to 250°C , and the control unit should provide two relay set points interface over the measured pressure range.

For the UHV range, two types of gauges are in common use on the accelerators around the world: cold cathode gauges and hot cathode gauges.

The hot cathode gauge needs a third gauge to cover readings between 10^{-3} and 5×10^{-4} mbar, also the hot cathode gauge has a filament which could burn in case of vacuum failure, but this is not the case with the cold cathode gauges, also it has a high outgassing in comparison with the cold cathode gauge.

For the cold cathode gauges, penning discharge cold cathode gauge does not cover pressure values below 10^{-9} mbar, while inverted magnetron discharge cold cathode gauge covers pressure ranges from 10^{-3} down to 10^{-11} mbar.

For all of the previous reasons, inverted magnetron cold cathode gauge (IMG) seems the best choice for SESAME, the gauge head should be bakeable to 250°C , and each gauge control unit should be able to operate at least two inverted magnetron and two Pirani gauges or 3 IMG and a Pirani.

Each part of the accelerator must be covered by a pressure gauge. In general, each vacuum section (area between two gate valves) should contain two pairs of total pressure gauges. A pair of total pressure gauge is also required for the Microtron, RF cavity, injection straight section, injector vacuum system, roughing stations, all should have at least one pair of total pressure gauges.

The location of the gauge need to be selected in a way which guarantees that there isn't any exposure to mechanical or magnetic noise and as far as possible from radiation which could destroy the electronics of the gauges. For SESAME the gauges are going to be installed near the first or the second crotch absorbers, a remark could be pointed out that the gauges will be close to the lumped pump which have a high pumping speed, so the gauges may not give the right reading of the pressure. The reason for the selection of this location that even that the gauge is close to high pumping speed but it is also close to the places with high outgassing, and in order to identify the pressure in the rest of the cell and to get a complete pressure profile, the voltage and current of the ion pumps will be used to identify the pressure, and this was the main reason of using only two total pressure gauges per cell. [13], [14]

7.8.2 Partial Pressure Gauges

It is important for UHV applications to know the composition of the residual gases within the system. Quadrupole mass spectrometer used as Residual Gas Analyser (RGA) measures the partial pressure of the gases in the system will be used for SESAME.

At least one RGA is required for each part of the accelerator (i.e. one RGA per vacuum cell); also at least one is required for the Microtron, the injector vacuum system, the injection straight section, the RF cavity and the ID straight section. In order to cover the rest of the machine it is recommended to have a to have blank flanges separated from the machine by all metal valves, where residual gas analysers can be installed when there is a need for that. Such fanges are going to be useful for other vacuum requirements and applications.

The heads should be bakeable to 250°C, and the RGA should cover a range between 0-200 AMU, however, residual gas analysers which cover up to 100AMU only can be used as they are cheaper than those cover up to 200AMU (also it is unusual to get gases in the system with masses higher than 100AMU), but (and just be to in the safe side) at least one must cover to 200AMU and it could be used as a portable RGA.

More detailed specifications for the RGA heads and control units will be issued in the future.

Control units of all the gauges and the other vacuum equipments need to be provided with all necessary cables, interlocks, front panels... etc, and they should have the ability to influence the main control system. [13]

Figure (7.7) shows a vacuum flow diagram for one cell of SESAME (1/4 of the storage ring). This diagram shows the locations of the pumps, gauges and the valves. These locations are optimised to have better vacuum performance.

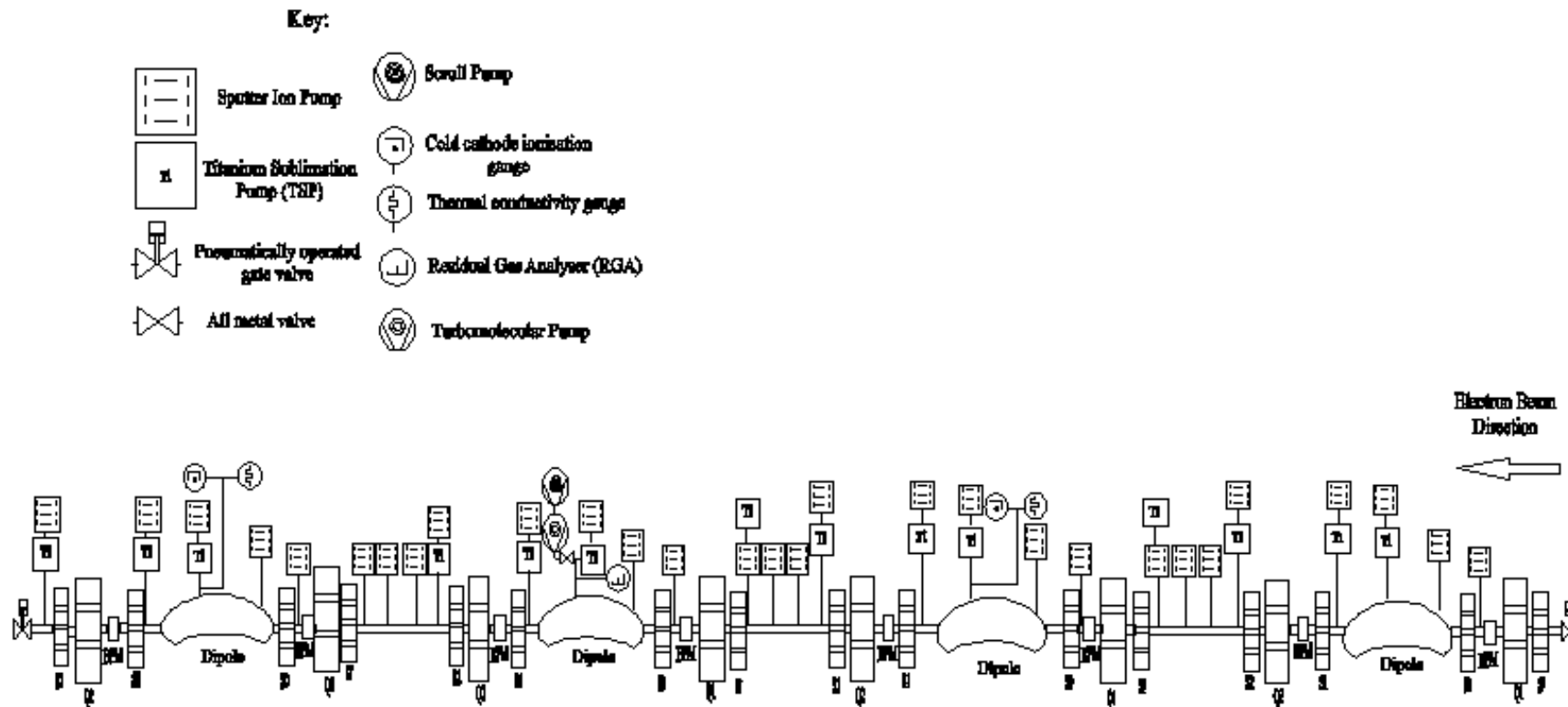


Figure 7.7: SESAME vacuum flow diagram (gauges, pumps and valves types and locations)

7.9 Cleaning, Bakeout and Infrastructure.

The decision was made not to bakeout in situ in order to cut the cost of the heaters, insulation and most importantly the size of the magnets will be smaller, so cheaper magnets will be used. A careful and a good preparation of the vacuum components before installation is required in order to reach the target pressure.

All components need to be cleaned properly. Cleaning procedures must guarantee that all components will be suitable for UHV. Cleaning will reduce the evolution of the gases from the surfaces; the source of these gases can be oils, greases, fluxes, fingerprints...etc. Cleaning should be suitable for the material type and should not leave any deposits behind. [15]

Many factors will decide the cleaning procedure; the target pressure, the material to be cleaned, safety regulations, cost...etc.

The cleaning procedure has been described for many materials for UHV application in many literatures, for SESAME and as stainless steel is the material of the vacuum chamber, then the following procedure is proposed in reference [15] to reach the required pressure:

1. Wash with a high pressure hot water (80°C) mixed with mild alkaline detergent.
2. Wash with hot water only to remove the detergent.
3. Drying the component with a blower of dry clean hot air.
4. Immerse completely in ultrasonic bath of clean hot solvent for 15 minute.
5. Leave the component in the vapour (the pure state) of the solvent for 15 minute.
6. Wash with demineralised pressurised hot water.
7. Immerse in a hot alkaline degreaser with ultrasonic agitation for 5 minutes.
8. Wash with demineralised pressurised hot water.
9. Dry with clean dry air.

After the cleaning, the components need to be baked under vacuum to 250°C for at least 24 hours to desorb water molecules, followed by vacuum firing at 950°C under 10^{-5} mbar vacuum.

It is very important to mention that care needs to be taken during the cleaning, as some chemicals are toxic.

Such a procedure is essential for all components facing vacuum, however, the cost is an important issue for SESAME, [for large parts (e.g. the dipole vacuum chamber) this will require large cleaning tanks and large ovens, which means high cost]. The solution for this is to follow the cleaning procedure in SESAME facility for only small parts, but for large contaminated parts need cleaning they need to be sent for cleaning and bakeout in specialised companies for cleaning, and have a spare parts of these vacuum chambers which have been cleaned, baked and stored under vacuum for the use when the contaminated large parts are in cleaning. Another approach being followed in some laboratories (e.g. SLS) is to depend more on long bakeout periods (which required large ovens or oven modules) without having a large cleaning facility.

The machine need to be supplied with dry nitrogen for use if venting of the machine is required, and the specification of the cleanliness and the humidity level of the nitrogen need to be investigated carefully, as this have a big impact in the outgassing rates of the different parts.

Compressed air is also required for the successful operation of the gate valves, the compressed air should be clean and at a pressure of 8bar. Helium is also required for leak chasing purposes. [16], [12]

A vacuum laboratory is required in the SESAME facility; there must be (in addition to the cleaning facility) a place for assembling and handling and clean rooms, also a storage is required.

It would be important to have a mechanical workshop in the early stages of the operation, as such a workshop with well-trained technicians will provide the facility with maintenance and the required components, and that will reduce the running cost of the machine.

7.10 Assembly

The assembly procedure is an important issue from vacuum point of view, the pumps and the vacuum chamber must be supplied stored under vacuum, and when they are assembled to the machine, they should not be exposed to atmosphere except after let up by dry nitrogen and after that they should not exposed to atmospheric air for long time, as the longer they exposed to air, the longer it will take to be pumped down. The assembly need to be done under a tent filled with nitrogen to guarantee the shortest possible pumping time.

7.11 Pressure Profile Calculations

In order to reach a good lifetime in the storage ring; the average pressure must be as small as possible. The average pressure is defined by the location of the pumps, the pumping speed, the outgassing of the vacuum chamber and the cross section of the vacuum chamber and profile.

For the optimisation of the location of the pumps and the pumping speed; the pressure profile calculations have to be performed.

The evaluation of the pressure profile can be done in several ways; one of the possible ways is by using Monte-Carlo Simulation. To use the simulation, the full detailed geometry of the vacuum chamber need to be designed, unfortunately the complete detailed design of SESAME is not finalised yet, so the estimation of the pressure profile will be done analytically by using a program written in MathCAD by Dr. Oleg Malyshev from SRS at CCLRC Daresbury Laboratory-UK.

The calculations will be performed based on the gas dynamic balance equation inside a vacuum chamber, equation (7.1), [17]

$$V \frac{dn}{dt} = q - cn + u \frac{d^2n}{dL^2} \quad (7.1)$$

Where:

V is vacuum chamber volume,

n is the gas density,

u is the specific vacuum chamber molecular gas flow conductance per unit axial length.

L is the longitudinal axis of the vacuum chamber,

c is the distributed pumping speed,

q the gas desorption flux from both thermal desorption and photo stimulated desorption, given by equation (7.2).

$$q = \eta_t F + \eta_\gamma \Gamma \quad (7.2)$$

Where:

F is surface area.

Γ is the photon flux.

η_t, η_γ are the thermal and photo stimulation desorption yields.

A detailed discussion along with the solution of this equation is presented in reference [17].

7.11.1 Gas Load Generation and Desorption Processes

The outgassing process controls the gas composition and the ultimate pressure achieved in the system.

In the storage ring the synchrotron radiation impinging the vacuum chamber walls and the absorbers producing a strong outgassing and thus increasing the dynamic pressure.

There is two discrete desorption processes: the thermal desorption and the photon stimulated desorption.

7.11.1.1 Thermal Desorption

All the materials facing vacuum desorbs gas into the system; the thermal desorption will define the base pressure of the system without synchrotron radiation.

The thermal desorption q_{th} can be evaluated by multiplying the total surface area (around $2.5 \cdot 10^6 \text{ cm}^2$) by the thermal outgassing rate of the material, ($\eta_t = 10^{-11} \text{ mbar.L/sec.cm}^2$). The areas need to be included in the calculations are all the areas facing vacuum, i.e. the vacuum chamber, the antechamber, the beam lines (up to the first valve to the front ends) and the pumping ports. As a result the expected thermal desorption load to be $2.7 \cdot 10^{-5} \text{ mbar.L/s}$.

It is important to mention that in order to reduce the thermal outgassing, baking out the different components to 250°C before installation is important, also decreasing the water contents on the surface could be reduced by using dry nitrogen for letting up the chamber in case of venting of the system as nitrogen desorbes much more easily than other gases. [18]

7.11.1.2 Photon Stimulated Desorption (PSD)

Photon stimulated desorption occurs when photons interact with the vacuum chamber surface producing photoelectrons which in its turn produce the desorption of the molecules by the electron stimulated desorption.

The quantity in interest is the photon induced gas desorption yield (η) which is the number of desorbed gas molecules per induced photon which decreases with the photon dose proportionally, $D^{-\alpha}$, where α varies from $2/3$ to 1 . For the calculations α will be used as $2/3$ as this value will give higher PSD and for not in situ baked vacuum chamber, as this will be the case for SESAME.

Figure (7.8) shows the experimental results of the variation of η with the beam dose (photon flux by the time) for CO (mass 28) for unbaked in situ and baked in situ vacuum chamber.

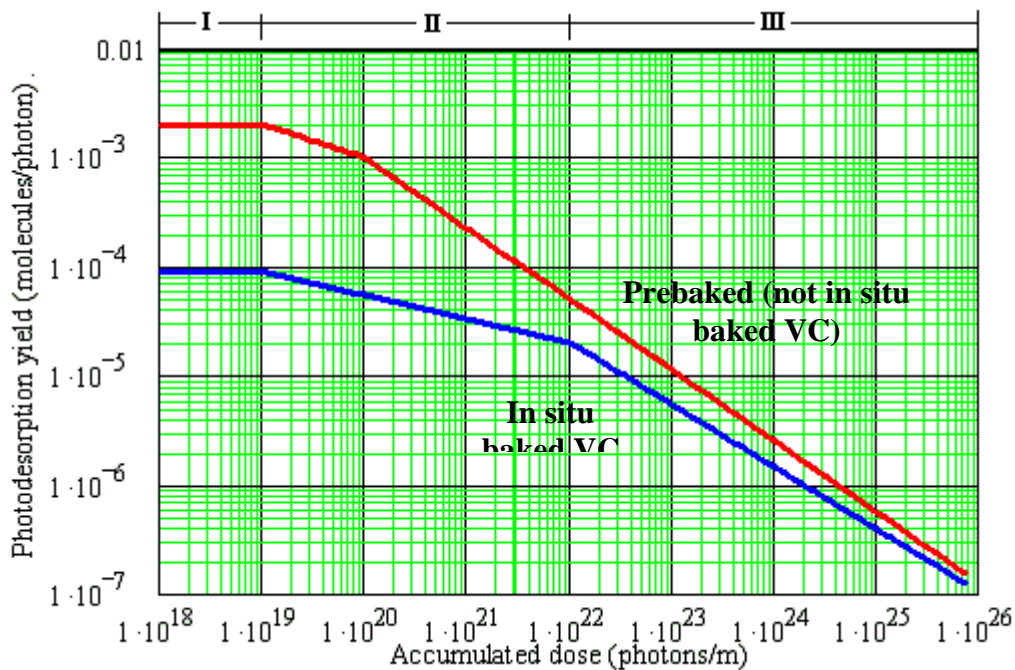


Figure 7.8: Photon stimulated desorption yield for CO (AMU 28) for in-situ baked and for prebaked vacuum chamber.

For the calculation purposes the curve have been divided into 3 regions, based on the slop of the curve, equation (7.3) shows the value of η based on the dose value.

$$\eta = \begin{cases} 0.002 & D \leq 10^{19} & \text{I} \\ 0.002 \left(\frac{10^{19}}{D}\right)^{0.3} & 10^{19} < D \leq 10^{20} & \text{II} \\ 2 \times 10^{-3} \left(\frac{10^{20}}{D}\right)^{0.65} & \text{otherwise} & \text{III} \end{cases} \quad (7.3)$$

7.11.2 Photon Flux from the Dipole

For the calculation of the photon stimulated desorption, the photon flux from the dipole need to be evaluated.

The radiation from the dipoles will find its way into 3 possible places: 1) to the crotch absorber 2) to the beam line front ends 3) It irradiates the walls of the vacuum chamber, however SESAME is being designed in a way that almost all unused synchrotron radiation to be absorbed by 4 lumped absorbers after each bending magnet, see figure (7.9).

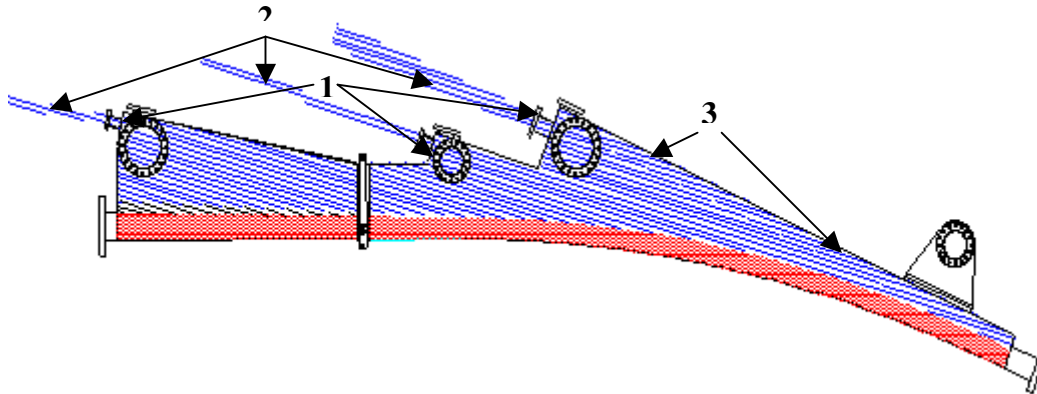


Figure 7.9: The expected way of the radiation; 1- to the absorber, 2- to the front ends, 3- to the walls.

Equation (7.4) has been used to evaluate the total photon flux (photons/sec) from the dipoles, [1] where with beam energy of 2.5GeV and 400mA beam current, the value of Γ is $8.042 \cdot 10^{20}$ photon/sec.

$$\Gamma_{\text{tot}} = 8 \cdot 10^{17} \cdot E \cdot I \quad (7.4)$$

So the contribution from each dipole is $5.027 \cdot 10^{19}$ photons/ sec. dipole.

Equation (7.5) shows the photon flux per metre length of the vacuum chamber (photons/m.s).

$$\Gamma(L) = \Gamma_{\text{rad}} \cdot \frac{(R_d + a) \sqrt{L^2 + 2R_d \cdot a + a^2} - LR_d}{\left[(R_d + a)^2 + L^2 \right] \sqrt{L^2 + 2 \cdot R_d \cdot a + a^2}} \quad (7.5)$$

Where:

$\Gamma(L)$ is the photon flux (photon/m.s) at L length from the dipole.

a is the long radius of the elliptical vacuum chamber.

Γ_{rad} is the angular photon flux (photon/rad.s), $\Gamma_{rad}=1.28 \cdot 10^{20} \cdot E \cdot I$

R_d is the bending radius.

The description of the different parameters being used in this equation is shown in figure (7.10).

Figure (7.11) shows the photon flux distribution along the dipole ($2.0 \cdot 10^{19}$ photon/s.m) and along the straight section, the minimum value for the photon flux is just before the following dipole magnet with a value of ($1.5 \cdot 10^{17}$ photon/s.m)

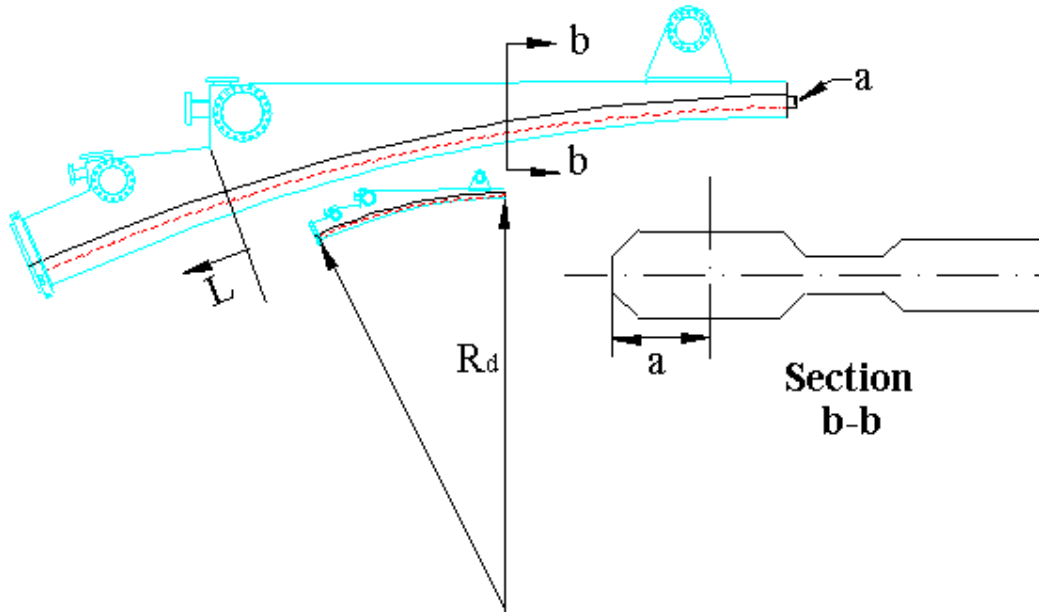


Figure 7.10: Description for the parameters in equation (7.5).

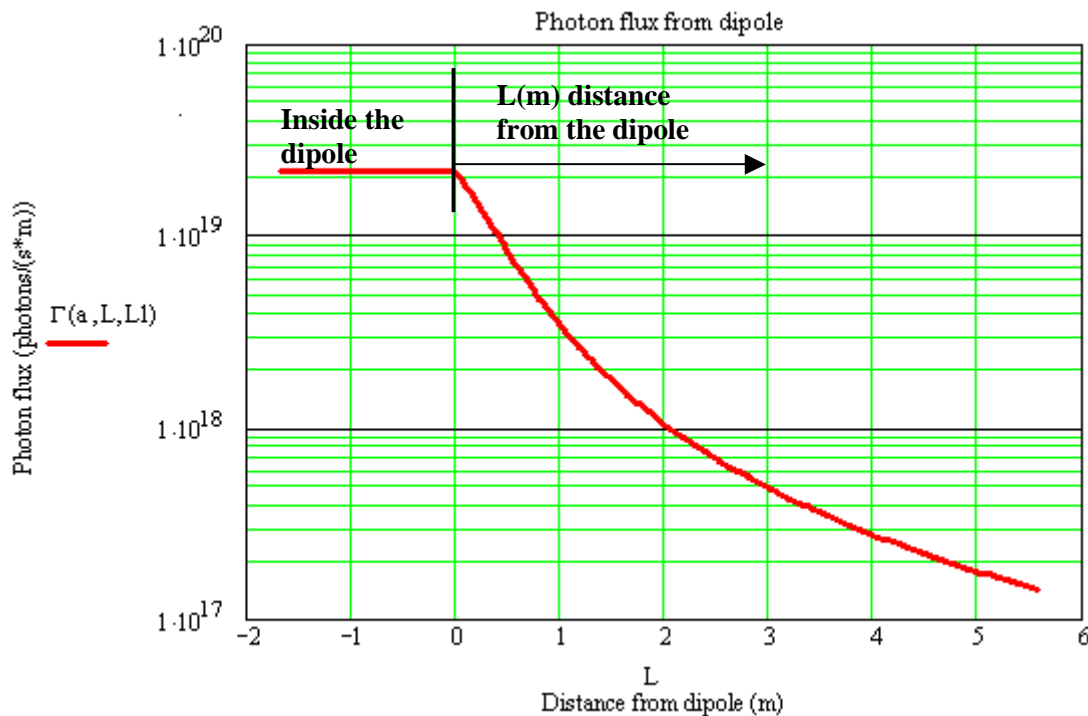


Figure 7.11: The photon flux from the dipole per metre distance from the dipole magnet.

7.11.3 Photon Stimulated Desorption Yield for SESAME (PSD)

As the photon stimulated desorption yield varies with the dose, and as the dose varies with photon flux which is variable with the distance from the dipole, then the value of the photon stimulated desorption yield will also vary with the distance. Figure (7.12) shows the photon stimulated desorption yield variation with the distance from the dipole for different conditioning time (dose rate). As it is shown in the figure, the PSD yield is maximum during the first stages of the conditioning process (around $4 \cdot 10^{-3}$ molecules/photon), and as the beam cleaning process for the vacuum chamber increase (at higher doses) the value will decrease until a value in the range of 10^{-5} molecules/photon being achieved after 100Ah beam dose, and this will decrease more and more for higher doses.

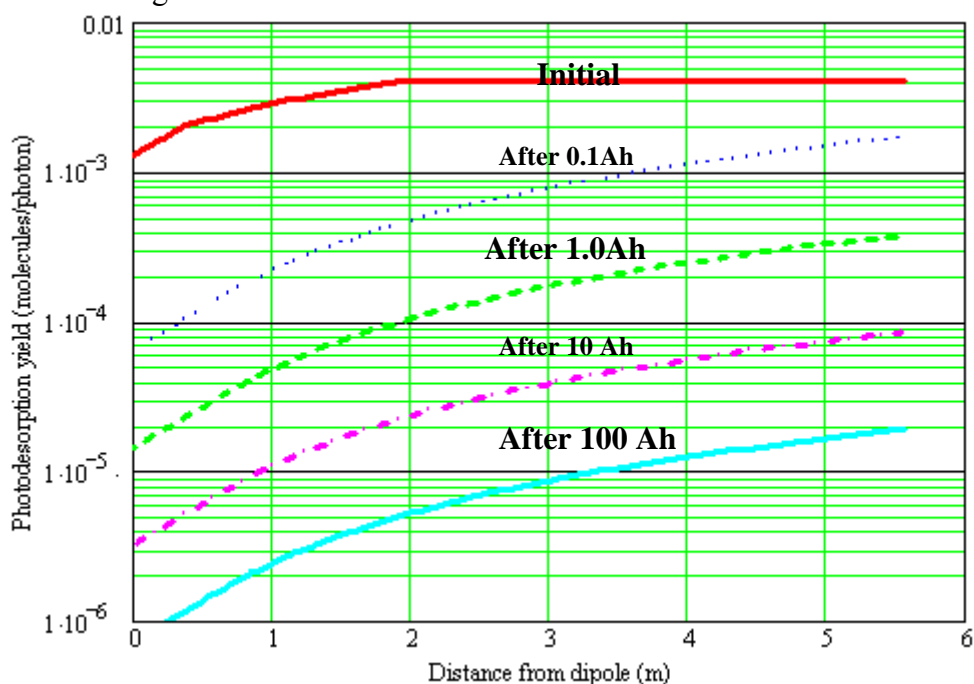


Figure 7.12: Photon stimulated desorption yield variation with distance from the dipole magnets for different beam dose.

7.11.4 Desorption Flux

The desorption flux (molecules/s.m) can be simply achieved by multiplying the photon stimulated desorption yield by the photon flux which both are function of the distance from the dipole. This will be the case also for the desorption flux, therefore the desorption flux variation with the distance is shown in figure (7.13), the curves are the multiplication of the curve in figure (7.11) and the curves in figure (7.12).

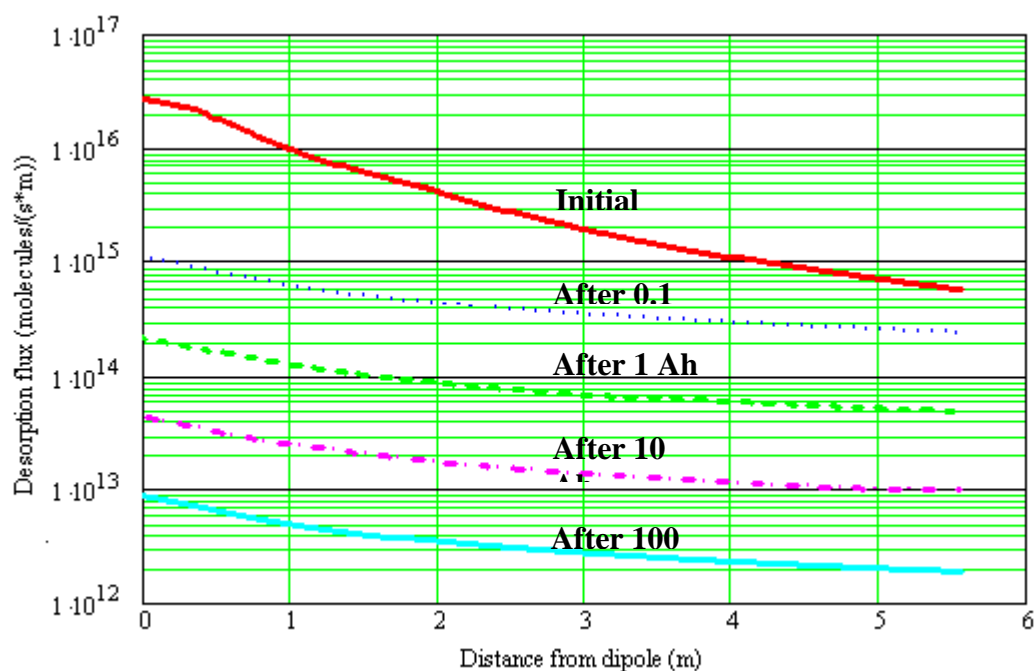


Figure 7.13: Desorption flux variation with the distance from the dipole for different beam dose.

7.11.5 The Achromat Pressure Profile

The following step in the calculations is to evaluate the pressure profile along the achromat, from both the thermal desorption which will give the base pressure “without beam” and the photon stimulated desorption which will give the dynamic pressure “with the beam”.

To evaluate the pressure profile the vacuum chamber achromat has been divided into parts, each part is defined by its length, if it is a pumped part or not, and the type and amount of pumping. Also it will be defined by the amount of photon flux it will get, and if it has an antechamber or not.

Table (7.2) shows part of the databases for the vacuum chamber of SESAME. l is the length of the section, L is the accumulated length from the beginning of the achromat, x is half the horizontal dimension of the vacuum chamber in the centre, and y is half the vertical dimension of the vacuum chamber measured at the centre.

Table 7.2: Part of the database of the SESAME achromat for the pressure profile calculations, the vacuum chamber is divided into sections for the calculation purposes.

ACHROMAT VACUUM CHAMBER ELEMENTS							
I (mm)	L (mm)	X (m)	Y (m)	Pumping	Photons	Antechamber (m)	Element
100	100	0.035	0.015	1	Distributed flux	0.1	Pump
867.5	967.5	0.035	0.015	0	Distributed flux	0.1	VC
150	1117.5	0.035	0.015	0	Distributed flux	0.1	Absorber +pump
50	1167.5	0.035	0.015	0	Distributed flux	0.1	Absorber
100	1267.5	0.035	0.015	4	Lumped absorber	0.1	Absorber
725	1992.5	0.035	0.015	0	Distributed flux	0	VC
230	2222.5	0.035	0.015	1	Distributed flux	0	Pump
420	2642.5	0.035	0.015	0	Distributed flux	0	VC
195	2837.5	0.035	0.015	0	Photons from the dipole VC	0.045	Dipole
300	3137.5	0.035	0.015	1	Photons from the dipole VC	0.1	Pump
1300	4437.5	0.035	0.015	0	Photons from the dipole VC	0.315	Dipole
150	4587.5	0.035	0.015	2	Photons from the dipole VC	0.395	Absorber +pump
394	4981.5	0.035	0.015	0	Photons from the dipole VC	0.26	Dipole
100	5081.5	0.035	0.015	2	Lumped absorber	0.3	Absorber +pump
48	5129.5	0.035	0.015	0	Distributed flux	0.31	VC
298	5427.5	0.035	0.015	0	Distributed flux	0.197	VC
812	6239.5	0.035	0.015	0	Distributed flux	0.34	VC
185	6424.5	0.035	0.015	3	Lumped absorber	0.378	Absorber +pump
188	6612.5	0.035	0.015	0	Distributed flux	0	VC
150	6762.5	0.035	0.015	0	Distributed flux	0.1	VC
100	6862.5	0.035	0.015	1	Distributed flux	0.1	Pump
958.5	7821	0.035	0.015	0	Distributed flux	0.1	VC
100	7921	0.035	0.015	1	Distributed flux	0.1	Pump
958.5	8879.5	0.035	0.015	0	Distributed flux	0.1	VC

7.11.5.1 Pumps Pumping Speed and the Average Dynamic Pressure

With these inputs and with nominal pumping speed for the pumps as follow (see figure (7.1)):

- Pump close to the 1st and 2nd absorber (indicated as 2 in the pumping column in the above table), nominal pumping speed for the ion pump= 300 L/s, the ion pump is combined with TSP with total expected pumping speed of 600L/s.
- Pump close to the 3rd absorber (indicated as 3 in the pumping column in the above table), nominal pumping speed for the ion pump= 500 L/s, the ion pump is combined with TSP with total expected pumping speed of 800L/s.
- Pump close to the 4th lumped absorber (indicated as 4 in the pumping column in the above table), nominal pumping speed for the ion pump= 300 L/s.
- All other pumps in the achromat with a nominal pumping speed for ion pumps= 150 L/s (indicated as 1 in the pumping column in the above table).

The total nominal pumping speed of the ion pumps for the storage ring is around 32,000 L/s.

From the above, the average base pressure was calculated with a value of: $P_{av,T} = 3.617 \cdot 10^{-10}$ mbar, and the average total pressure is: $P_{av} = 1.81 \cdot 10^{-9}$ mbar.

Figure (7.14) shows the base pressure profile (due to thermal desorption / without SR beam) and the dynamic pressure (due to both the thermal and the photo stimulated desorption / with SR beam) at 100Ah and beam current of 400mA.

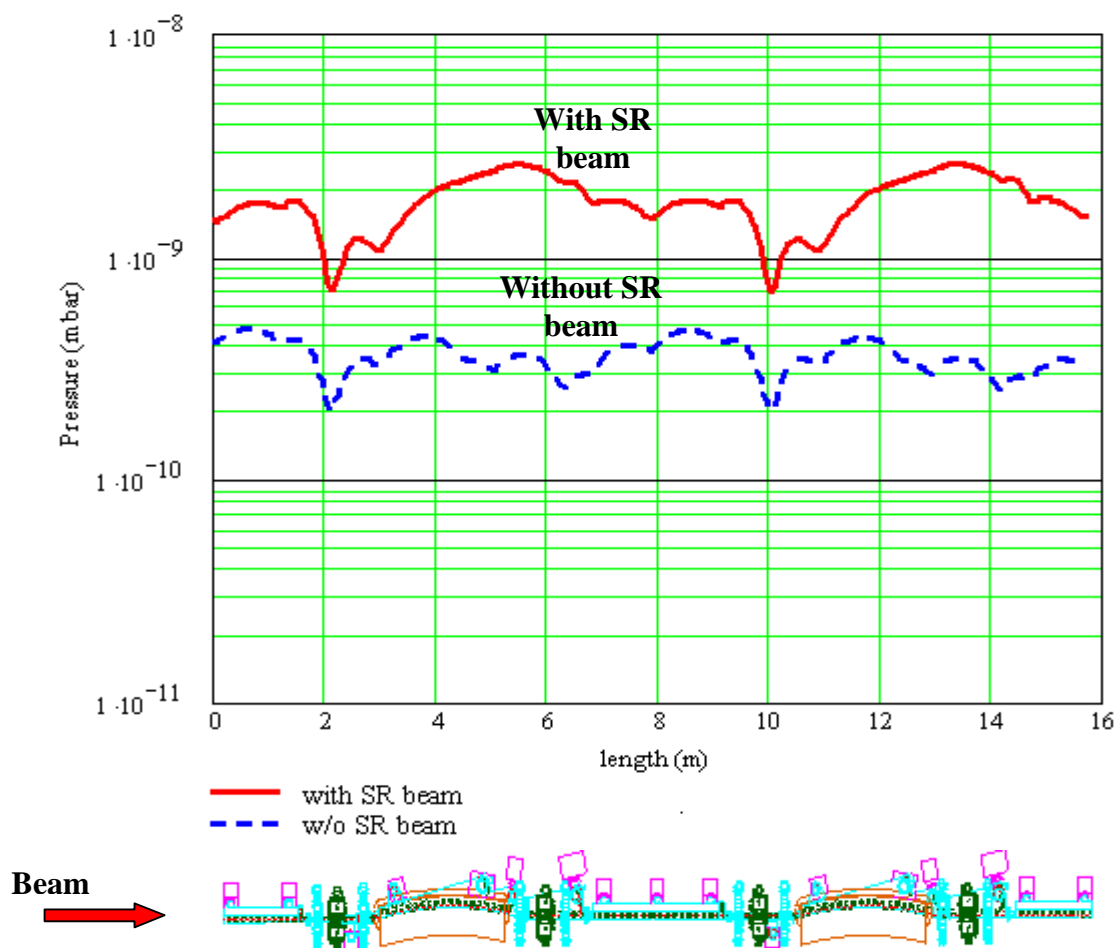


Figure 7.14: Pressure profile for 1/8 of the storage ring, $P_{av,T} = 3.617 \cdot 10^{-10}$ mbar, $P_{av,PSD} = 1.443 \cdot 10^{-9}$ mbar, $P_{av} = 1.81 \cdot 10^{-9}$ mbar, at 100Ah, 400mA.

The behaviour of the pressure profile curve is as it is expected; the highs and lows of the curve represent places without pumps and with high outgassing and places with pumps, respectively. The highest values of the pressure were in places with high outgassing rates; i.e. in the dipoles and close to the crotch absorbers, the maximum value for the pressure at these areas is: $P_{av} = 2.62 \cdot 10^{-9}$ mbar, and the lowest values is just before the following dipole (in the pre-dipole area) as this location is the area which has the lowest outgassing rate, the average total pressure in the pre-dipole is $P_{av} = 6.9 \cdot 10^{-10}$ mbar.

7.11.5.2 Changes in the Pumps Pumping Speed and the Average Dynamic Pressure Achieved.

Some changes with the pumping speed could help in achieving better vacuum, for example increasing the pumping speed for the pump close to the third absorber into 1000L/s will reduce the pressure with a value for the dynamic average pressure of $P_{av} = 1.644 \cdot 10^{-9}$ mbar. With the pumping speed of the first and second absorber changed into 500L/s (see figure (7.1)) and for that of the third absorber of 1000L/s, the pressure will reduce into $P_{av} = 1.452 \cdot 10^{-9}$ mbar.

However, the cost of such pumps is high, so keeping the pumping speed of the ion pumps as mentioned in section 7.11.5.1 is proposed with the need of the additional pumping speed from TSP. The average dynamic pressure will be reduced due to beam cleaning of the vacuum chamber as discussed in the following section.

7.11.5.3 Average Dynamic Pressure of the Achromat During Commissioning and Operation of the Machine.

Table (7.3) shows the expected average dynamic pressure values for the same design and pumping speed for the pumps (in section 7.11.5.1), for (2.5GeV and 2GeV) beam energies and (200mA and 400mA) beam currents at different dose.

Table (7.3): The variation of the average dynamic pressure (mbar) with the beam dose, beam energy and beam current.

Dose (Ah)	Beam Energy and Beam Current			
	2.5 GeV and 400mA	2.0 GeV and 400mA	2.5 GeV and 200mA	2.0 GeV and 200mA
Initial	$1.865 \cdot 10^{-6}$	$1.55 \cdot 10^{-6}$	$1.03 \cdot 10^{-6}$	$8.38 \cdot 10^{-7}$
100	$1.805 \cdot 10^{-9}$	$1.625 \cdot 10^{-9}$	$1.08 \cdot 10^{-9}$	$9.93 \cdot 10^{-10}$
200	$1.496 \cdot 10^{-9}$	$1.34 \cdot 10^{-9}$	$9.29 \cdot 10^{-10}$	$8.49 \cdot 10^{-10}$
300	$1.373 \cdot 10^{-9}$	$1.22 \cdot 10^{-9}$	$8.70 \cdot 10^{-10}$	$7.92 \cdot 10^{-10}$
400	$1.305 \cdot 10^{-9}$	$1.16 \cdot 10^{-9}$	$8.34 \cdot 10^{-10}$	$7.61 \cdot 10^{-10}$
500	$1.261 \cdot 10^{-9}$	$1.12 \cdot 10^{-9}$	$8.11 \cdot 10^{-10}$	$7.41 \cdot 10^{-10}$
600	$1.23 \cdot 10^{-9}$	$1.087 \cdot 10^{-9}$	$7.91 \cdot 10^{-10}$	$7.22 \cdot 10^{-10}$
700	$1.207 \cdot 10^{-9}$	$1.066 \cdot 10^{-9}$	$7.80 \cdot 10^{-10}$	$7.10 \cdot 10^{-10}$

The estimated beam dose by the end of the commissioning stage of the storage ring is expected to be 400Ah, and the machine will run at 200mA in the beginning, so the estimated dynamic average pressure for that will be: $P_{av} = 8.34 \cdot 10^{-10}$ mbar, see figure (7.15). After a year of the end of the commissioning stage the machine will run at 400mA beam current and it will have an expected beam dose of 1000Ah, for these values the expected dynamic average pressure is $P_{av} = 1.161 \cdot 10^{-9}$ mbar, figure (7.16).

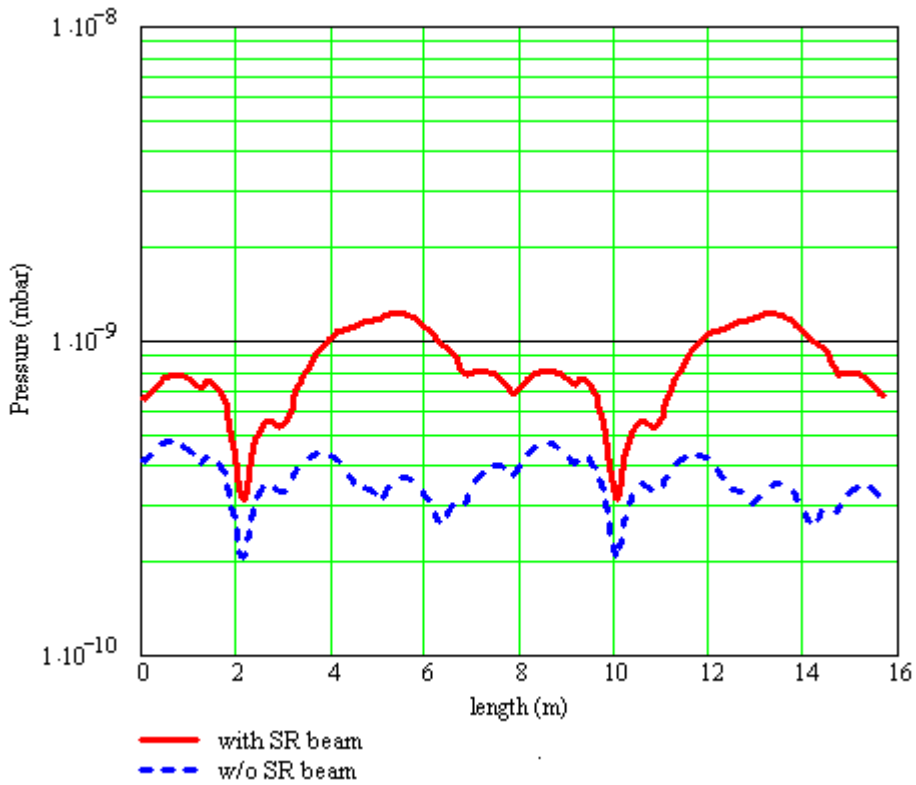


Figure 7.15: Pressure profile for 1/8 of the storage ring, $P_{av,T} = 3.617 \cdot 10^{-10}$ mbar, $P_{av,PSD} = 4.719 \cdot 10^{-10}$ mbar, $P_{av} = 8.336 \cdot 10^{-10}$ mbar, by the end of the conditioning stage of the machine.

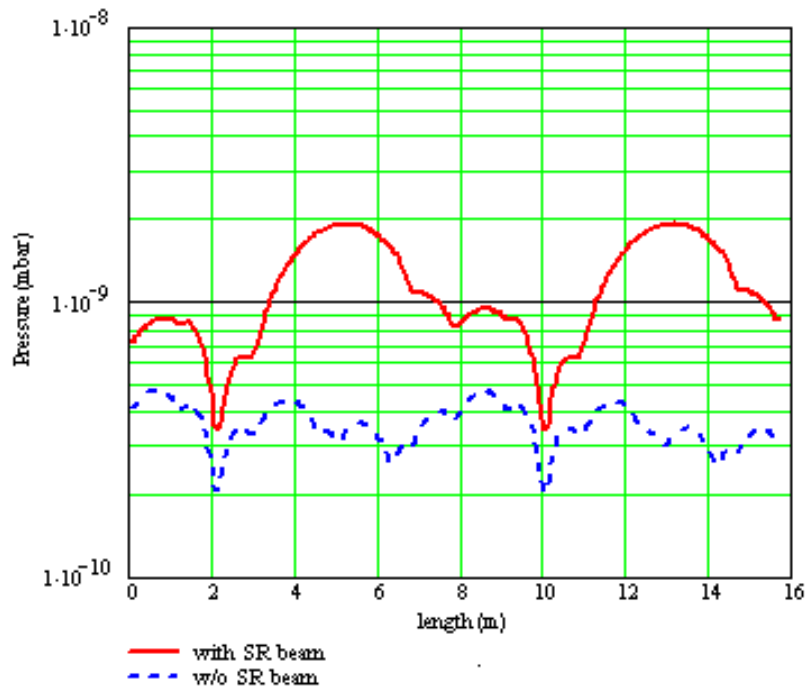


Figure 7.16: Pressure profile for 1/8 of the storage ring, $P_{av,T} = 3.617 \cdot 10^{-10}$ mbar, $P_{av,PSD} = 7.994 \cdot 10^{-10}$ mbar, $P_{av} = 1.161 \cdot 10^{-9}$ mbar, after a year of the end of the conditioning stage of the machine.

The main difference between the two curves that the machine will have a higher pressure after one year of its operation than that during the conditioning stage, the reason for this is that the machine will work with higher current (400mA) while during the conditioning stage the machine will run with half the operation current (200mA).

7.12 SESAME Microtron Vacuum System

BESSY I injection system will be upgraded to suit SESAME.

The old machine microtron used to be evacuated by using two turbomolecular pumps with one baking pump, in order to have a good vacuum there, the design will be changed by having two 200L/s ion pumps to replace the two turbomolecular pumps and a mobile roughing station consist of a baking pump and a turbomolecular pump will be installed via a valve in place of the old baking pump.

In addition, two pairs of total pressure gauges (consist of an IMG and a Pirani) will be used for total pressure measurement purposes. An RGA will be used also for partial pressure measurements.

A gate valve will be used to isolate the microtron from the rest of the machine.

References:

- [1] Oswala Grobner, “*Dynamic Outgassing*” CAS, 1999-Denmark.
- [2] Ron Ried, “*Materials Choice for Diamond Vacuum System*”, (Daresbury Laboratory Internal Report) Oct. 2000.
- [3] Erhard Huttel, “*Materials for Accelerator Vacuum System*”. CAS, 1999-Denmark.
- [4] Lothar Schulz, “*Stainless Steel Vacuum Chambers*” Oct. 2001.
- [5] Keith Middleman, Daresbury Laboratory, Privet communication.
- [6] SLS Handbook.
- [7] D. Lowe, “*CLS Storage Ring Vacuum Chambers*”, March 2001.
- [8] Keith Middleman et al. “*Rough Pumping Systems for Diamond Storage Ring, Part 1 and Part 2*”, (Daresbury Laboratory Internal Report) Oct. 2001.
- [9] Tom Weston, “*Capture pumps*”, Vacuum Design Notes, Feb. 1996.
- [10] Lothar Schulz, “*Sputter ion pumps*” CAS, 1999-Denmark.
- [11] Diamond International vacuum workshop, Sep. 2002.
- [12] *Diamond Synchrotron light source, Report of the design specifications*”, June 2002.
- [13] Joe Herbert, “*Vacuum Instrumentation for Diamond*”, (Daresbury Laboratory Internal Report) Jan 2002.
- [14] F. Daclon et al. “*Elettra Vacuum system, part 1*” July 1994.
- [15] Ron Reid, “*Cleaning for vacuum services*”, CAS, 1999-Denmark.
- [16] Keith Middleman et al, “*Service Requirements for the Diamond Machine Complex*”,(Daresbury Laboratory Internal Report).
- [17] Oleg Malyshev et al. “*Calculated Pressure profile Along the Diamond Storage Ring Cell.*” (Daresbury Laboratory Internal Report) Jan 2002.
- [18] Karl Jousten, “*Thermal Outgassing*” CAS, 1999-Denmark.